Raman Optical Activity. Computation of Circular Intensity Differentials for Bromochlorofluoromethane

P. L. Prasad[†] and D. F. Burow*

Contribution from the Bowman-Oddy Laboratories, Department of Chemistry, University of Toledo, Toledo, Ohio 43606. Received May 8, 1978

Abstract: The Raman optical activity (ROA) parameters for bromochlorofluoromethane have been calculated using an atom–dipole interaction (ADI) procedure. Raman intensities were measured in both liquid and vapor phases and molecular polarizability derivatives were determined. These Raman scattering parameters along with previously developed molecular force fields were used to evaluate the circular intensity differentials (CIDs) for all fundamental vibrational modes of (R)-HCBrClF and (R)-DCBrClF. The predicted CIDs range from 10^{-5} to 10^{-3} with those for deformation modes being larger than those of stretching modes. Thus, these results are consistent in magnitude and mode type dependence with results reported on other molecules. Furthermore, the sign pattern of the CIDs of the three low-frequency modes of HCBrClF corresponds directly to the CIDs reported for the skeletal deformation modes of α-phenylethyl isocyanate. These results will serve as a model for the CIDs of other molecules where motion about an asymmetrically substituted carbon atom occurs.

Introduction

Raman optical activity (ROA)[1] and infrared vibrational circular dichroism (VCD)[2] have been reported for a variety of optically active compounds. In ROA, the larger circular intensity differentials (CIDs) have been observed in skeletal or C–H deformation modes of phenyl-substituted ethanes,[3,4] terpenes,[5] camphors,[6] sulfoxides,[7] and tartaric acid derivatives.[8] Diem et al.[9] have found that, in favorable situations, carbon–halogen stretching modes also exhibit appreciable CIDs, probably via coupling with skeletal deformation modes since a conformer dependence was apparent. VCD has been limited by instrumentation to high-frequency modes where circular dichroism has been observed in C–H, C–D, and O–H fundamental stretching modes[2,10] and in several overtone and combination modes.[11] Fixed partial charge,[12-14] polar tensor,[14] and coupled oscillator models[15] have been developed in an attempt to predict or correlate the VCD results. In recognition of the necessity of a guide for observation and interpretation of ROA, we presented[16] an atom–dipole interaction (ADI) model for computation of Raman CIDs. Here we apply this model to the molecule bromochlorofluoromethane (HCBrClF) and its deuterated analogue.

There are several reasons behind our choice of HCBrClF for initial application of the ADI model for Raman optical activity. First, HCBrClF is one of the simplest optically active molecules available in the laboratory so that comparison between prediction and observation is feasible. The complexity of the computation precludes full treatment of large molecules at this stage. Secondly, data needed for the computation are available: we have developed[17,18] both Urey–Bradley and general valence force fields; structural[17] and atomic polarizability parameters[19,20] are also available. Finally, Marcott et al.[14] have predicted the infrared VCD of HCBrClF in both the fundamental and binary combination modes so that a direct comparison of both chiroptical effects in the same molecule is possible.

In this paper we present data on the vapor- and liquid-phase Raman intensities of HCBrClF and DCBrClF. Next we utilize these gas-phase intensities along with previously reported depolarization ratios,[17] force fields,[17,18] and atomic polarizabilities[19,20] to optimize the polarizability derivative tensors for the constituent atoms, via the ADI model. Finally we compute the Raman CIDs from these optimized tensors with the techniques discussed in the preceding article.[16]

Experimental Section

Raman spectra were measured using a spectrometer and techniques described elsewhere.[17] A 488-nm Ar⁺ laser line was used for excitation; 1.2 W (double pass) was used for vapor-phase and 0.45 W (single pass) was used for liquid-phase measurements. Spectral slit widths of ca. 5 (vapor phase) and ca. 4 cm^{-1} (liquid phase) were employed. A photon counter (Princeton Applied Research Model 1110) was used to measure intensities. Data were recorded on paper tape and integrated off-line using Simpson's numerical integration. All intensities were measured at least twice in successive scans of the spectrum.

Vapor-phase samples were made up in a large sample bulb with mechanical stirring; pressures were measured with a Wallace Tiernan gauge. Methane–nitrogen mixtures were used to check our intensity measurements. The samples of HCBrClF and DCBrClF were taken from the same material used for spectral studies reported earlier. For HCBrClF, 272 Torr of sample was diluted with 481 Torr of N_2 to provide an internal reference. A similar pressure of DCBrClF was utilized but the small quantity of sample and large vacuum line volume precluded dilution with N_2. Since previous work indicated ν_9 to have the same intensity, similar depolarization ratios, and similar mode descriptions in both molecules, the spectrum of DCBrClF was scaled to that of HCBrClF by transferring the mean polarizability derivative for ν_9 of HCBrClF to its isotopically substituted molecule. For liquid-phase intensities, a small amount of CS_2 (2.4% by weight) was added to HCBrClF as an internal reference.

Raman Intensities

Measured values of integrated Raman intensities are converted to absolute scattering parameters by concurrent measurement of the intensity of one of the Raman bands of an internal reference compound. For the vapor phase, the ratio of intensities of sample (s) and reference (r) bands i and j, respectively, is expressed[21] by

$$\frac{I_i^s}{I_j^r} = \frac{M_s g_i f_i S_j}{M_r g_j f_j S_i} \left[\frac{\overline{\alpha_i}'}{\overline{\alpha_j}'}\right]^2 \frac{1+\rho_i}{3-4\rho_i} \frac{3-4\rho_j}{1+\rho_j} \tag{1}$$

where I is the integrated intensity, M is the concentration, g is the degeneracy of the vibration, S is the instrument response function, ρ is the depolarization ratio for linearly polarized incident light, and $\overline{\alpha}'$ is the mean polarizability derivative. In eq 1, f_i represents the quantity $(\nu_0 - \nu_i)^4/\nu_i[1 - \exp(hc\nu_i/kT)]$ where ν_0 is the excitation frequency and ν_i is the Raman shift.

Vapor-phase intensity measurements were calibrated by measuring the Raman band intensities of N_2 and CH_4 mixtures. By using the measured intensities of the ν_1 (2920 cm^{-1}) band of CH_4 and the 2330-cm^{-1} band of N_2 along with a value of 2.08 $Å^2$ amu$^{-1/2}$ for $\overline{\alpha}'_{2920}$,[22] we obtained a value of 0.59_7

Table I. Measured Raman Scattering Parameters[a] for Bromochlorofluoromethane

| | HCBrClF | | | | | | | DCBrClF | | |
| | liquid phase | | | vapor phase | | | rel bandwidth liq/vap | depol[b] ratio | vapor phase | |
	depol[b] ratio	$\bar{\alpha}'^2$	γ'^2	$\bar{\alpha}'^2$	γ'^2	$\alpha'_{liq}{}^2/\alpha'_{vap}{}^2$			$\bar{\alpha}'^2$	γ'^2
ν_1	0.12	3.37_6	7.2_3	0.75_7	1.6_2	4.4	9.3	0.12	$0.5_8{}^c$	1.2_5
ν_2	0.40	0.11_6	1.4_9	0.01_7	0.2_1	6.8	4.7	0.15	$0.1_8{}^c$	0.5_0
ν_3	0.30	0.08_5	0.6_4	0.01_0	0.07_8	8.2	11.5	0.24	$0.1_3{}^c$	0.6_9
ν_4	0.58	0.03_1	1.1_9	0.14_0	5.3_9	1/4.5	1.3	0.40	0.21_4	2.7_5
ν_5	0.61	0.04_7	2.2_9	0.23_8	$11._7$	1/5.9	1.1	0.35	0.60_4	5.9_5
ν_6	0.06	1.1_0	1.0_8	0.23_1	0.22_6	4.7	4.4	0.09	0.11_3	0.17_3
ν_7	0.07	0.30_3	0.35_0	0.07_4	0.08_6	4.1	5.8	0.07	0.04_7	0.05_4
ν_8	0.24	0.13_0	0.68_6	0.01_6	0.08_4	8.1	3.7	0.29	0.01_1	0.08_0
ν_9	0.23	0.15_5	0.76_9	0.02_2	0.10_8	7.1	2.8	0.24	0.02_2	0.11_5

[a] The square of the mean polarizability derivative, $\bar{\alpha}'^2$, and the anisotropy γ'^2 are in units of Å^4 amu^{-1}. [b] The depolarization ratio is for linearly polarized incident light; all values were measured for the liquid phase (ref 17). [c] These values have considerable uncertainty owing to experimental difficulties; see text.

Å^2 $\text{amu}^{-1/2}$ for $\bar{\alpha}'_{2330}$ of N_2. This compares favorably with the value of 0.62 Å^2 $\text{amu}^{-1/2}$ reported by Fontal and Spiro.[23]

Absolute intensities for vapor-phase HCBrClF were measured using the 2330-cm^{-1} band of N_2 as a reference. The intensity of ν_3 is somewhat uncertain owing to proximity with $\nu_5 + \nu_7$. As described in the Experimental Section, the band intensities of DCBrClF were scaled to those of HCBrClF. In DCBrClF, the measured intensity of ν_1 is somewhat uncertain owing to practical difficulties and overlapping overtone; combination bands precluded precision measurement of the intensities of both ν_2 and ν_3. The mean polarizability derivatives for both molecules are summarized in Table I. The anisotropy, $(\gamma')^2$, was calculated from the depolarization ratio of the liquid-phase Raman bands:

$$\gamma'^2 = 45\bar{\alpha}'^2\rho/3 - 4\rho \qquad (2)$$

Although vapor-phase scattering parameters are the only appropriate parameters for use in computation, it is recognized that measurement of ROA is restricted to the liquid phase. Intermolecular interactions in the liquid phase could produce significant differences in the ROA of gas- and liquid-phase samples. In anticipation of including corrections for medium effects at some future date and for identifying those modes where medium effects would be most prominent, we have also measured the Raman intensities of HCBrClF in the liquid phase.

The Raman scattering cross section $\partial\sigma_k/\partial\Omega$ in the liquid phase is believed[24] to be larger than that in the vapor phase owing to internal field effects:

$$\partial\sigma_k/\partial\Omega = \frac{(2\pi)^4}{45}\frac{h}{8\pi^2 c}\Delta I_k \qquad (3)$$

where I_k is the scattered intensity for the kth Raman band of the free molecule. Assuming that the refractive index of the liquid is the same for both incident and scattered frequencies, the local field factor Λ is given as

$$\Lambda = [(n^2 + 2)/3]^4 \qquad (4)$$

where n represents the refractive index of the liquid. Inclusion of field effects results in a modification of eq 1:

$$\frac{I_i^s}{I_j^r} = \frac{M_s g_i f_i S_j}{M_r g_j f_j S_i}\left[\frac{\bar{\alpha}_i'}{\alpha_j'}\right]^2 \frac{1 + \rho_i}{3 - 4\rho_i}\frac{3 - 4\rho_j}{1 + \rho_j}\frac{\Lambda^s}{\Lambda^r} \qquad (5)$$

The intensites of all Raman bands in liquid HCBrClF were measured with CS_2 as the internal reference. The intensity of the 660-cm^{-1} band of CS_2 was standardized with respect to the intensity of ν_1 of CCl_4 by using a value of 0.685 Å^2 $\text{amu}^{-1/2}$ for $\bar{\alpha}'_{459}$ of CCl_4,[25] obtained from $\partial\bar{\alpha}/\partial R_{C-Cl} = 2.04$ Å^2. Overlap of the CS_2 band and ν_6 of HCBrClF was accommo-

dated by making intensity measurements at several low concentrations of CS_2 in HCBrClF and assuming a linear dependence of intensity on concentration. Values of the liquid-phase scattering parameters for HCBrClF, calculated from eq 5, along with the corresponding gas-phase parameters are summarized in Table I.

A comparison between the scattering parameters (Table I) of liquid- and vapor-phase HCBrClF leads to several interesting observations. First of all, as expected from eq 3 and 4, all mean polarizability derivatives apparently increase upon condensation except for the C-F (ν_4) and C-Cl (ν_5) stretching modes. Secondly, the bandwidths increase substantially upon condensation, again with the exception of the C-F and C-Cl stretching modes. Thirdly, the bending modes exhibit larger changes in mean polarizability derivatives upon condensation than the stretching modes. Finally, in the liquid phase, the mean polarizability derivatives of the bending modes are *not* very small compared to those of the stretching modes. This observation is contrary to the general belief that stretching modes exhibit large changes in molecular polarizability and bending modes produce negligible changes. Since the gas-phase values of $\bar{\alpha}'^2$ do, however, follow this trend rather well, the deviations must be attributed to medium effects. Thus it is apparent that the bending modes are more substantially affected by the surrounding medium than are the stretching modes.
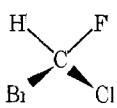
Since the same depolarization ratios were adopted for both gas- and liquid-phase CHBrClF, the ratios of Raman scattering cross sections and of mean polarizability derivative squares are expected to be equal to the field factor Λ. Supposedly Λ accounts for the medium effects; yet in HCBrClF a comparison of the $(\bar{\alpha}'_{liq}{}^2/\bar{\alpha}'_{vap}{}^2)$ ratios given in Table I for all Raman bands (with $\Lambda = 3.4$ for HCBrClF) does not seem to justify this supposition. Interestingly enough, the medium effects seem to be described empirically by separate values of the field factor for stretching and bending modes:

$$\Lambda \text{ (stretching)} = n\Lambda = n\left(\frac{n^2 + 2}{3}\right)^4 \qquad (6)$$

$$\Lambda \text{ (bending)} = (n + 1)\Lambda = (n + 1)\left(\frac{n^2 + 2}{3}\right)^4 \qquad (7)$$

The values predicted by these modified equations are seen to compare well with the $(\bar{\alpha}'_{liq}{}^2/\bar{\alpha}'_{vap}{}^2)$ ratios averaged separately for stretching and bending modes in HCBrClF. Furthermore, if the medium effects were inversely involved in ν_4 and ν_5 the observed decrease of $\bar{\alpha}'^2$ upon condensation in these modes would also be accommodated.

Although for our present purposes it is sufficient just to recognize that substantial intermolecular interactions prevail

Table II. Principal Cartesian Coordinates Used for (R)-Bromochlorofluoromethane[a]

	Cl	C	F	H	Br
X	0.0581	−0.4362	0.1603	−1.5565	0.0216
Y	−0.6952	0.4531	1.6403	0.5928	−0.1613
Z	1.8681	0.6393	0.8651	0.7215	−1.1283

[a] This structure (in units of Å) was derived from that in ref 17.

in liquid HCBrClF, it is useful, for future studies on intermolecular interactions, to summarize the novel features of the phase dependence of $\bar{\alpha}'^2$ for HCBrClF.

(a) Medium effects on $\bar{\alpha}'^2$ are dependent on the nature of vibrations.

(b) The magnitudes of $\bar{\alpha}'^2$ for bending modes are as high as, if not greater than, those for most of the stretching modes.

(c) Upon condensation, $\bar{\alpha}'^2$ for stretching modes ν_4 and ν_5 decreases.

Since these features are contrary to general belief, the need for further exploration of the dependence of Raman intensities on intermolecular interactions is obvious. Now this evidence for strong medium effects on the Raman spectrum leads us to speculate that HCBrClF may exhibit Raman CIDs which are also phase dependent.

Calculations and Discussion

Computation of Raman CIDs requires evaluation of the Cartesian derivative tensors of atomic polarizabilities $\nabla_X \alpha_i$, where

$$\nabla_X \alpha_i = \begin{bmatrix} \dfrac{\partial \alpha_i^{xx}}{\partial x_i} & \dfrac{\partial \alpha_i^{xx}}{\partial y_i} & \dfrac{\partial \alpha_i^{xx}}{\partial z_i} \\[2mm] \dfrac{\partial \alpha_i^{yy}}{\partial x_i} & \dfrac{\partial \alpha_i^{yy}}{\partial y_i} & \dfrac{\partial \alpha_i^{yy}}{\partial z_i} \\[2mm] \dfrac{\partial \alpha_i^{zz}}{\partial x_i} & \dfrac{\partial \alpha_i^{zz}}{\partial y_i} & \dfrac{\partial \alpha_i^{zz}}{\partial z_i} \end{bmatrix} \qquad (8)$$

These parameters are related directly to the Raman scattering parameters in the manner described in the preceding article.[16] For optimization of the $\nabla_X \alpha_i$ tensors, the Raman intensity and depolarization ratio data for the nine fundamental vibrations of HCBrClF alone are not sufficient. Since these tensors can be confidently considered to be isotopically invariant, the corresponding data for DCBrClF were used to provide the additional information. The uncertainty in the intensities of ν_1, ν_2, and ν_3 further limited the data to only six intensities and nine depolarization ratios for DCBrClF. Thus a total of 33 experimentally observed quantities were available for optimization of the 5 independent $\nabla_X \alpha_i$ tensors. Since this would involve 45 unknown parameters, optimization was not practical without resorting to approximation. In the preceding article,[16] we noted that exclusion of some contributions to the atomic polarizability derivative renders all elements in each column of $\nabla_X \alpha_i$ tensors equal. Although in such a case only 15 unknown quantities would need to be optimized, the resultant tensors may not yield a realistic description of the changes in the polarizability ellipsoids during molecular vibrations. As a compromise between these extreme cases, a symmetric $\nabla_X \alpha_i$ tensor was considered to give a fair representation of the distortions in atomic polarizabilities during molecular vibrations. In this situation each $\nabla_X \alpha_i$ tensor is described by six parameters and therefore 30 unknown parameters are to be optimized from 33 experimental quantities.

For optimization of the symmetric $\nabla_X \alpha_i$ tensors, an initial trial set of tensors was derived from the internal coordinate derivatives of atomic polarizability which Applequist and Quicksall[20] optimized for a set of halomethanes. The principal Cartesian coordinates of HCBrClF, derived from electron diffraction data, that were employed in the present calculations are summarized in Table II. The symmetric $\nabla_X \alpha_i$ tensors were then transformed to the normal coordinate derivatives $\nabla_Q \alpha_i$ through

$$\nabla_Q \alpha_i = \nabla_X \alpha_i \, \mathbf{DL} \qquad (9)$$

where $\mathbf{D}$, the inverse of Wilson's $\mathbf{B}$ matrix,[26] and $\mathbf{L}$, the eigenvector matrix of the vibrational secular equation, were obtained from our earlier vibrational analyses[17,18] of these molecules. From this initial set of $\nabla_Q \alpha_i$ parameters, the Raman scattering parameters for all modes of HCBrClF and DCBrClF were obtained from the following equation.

$$\alpha'_{mol} = -\mathbf{BC'B} \qquad (10)$$

Here α'_{mol} represents the molecular polarizability derivative tensor, $\mathbf{B}$ represents the relay tensor matrix, and $\mathbf{C'}$[27,28] represents the normal coordinate derivative matrix of the inverse of the relay tensor matrix. As described in the previous article,[16] the relay tensor matrix $\mathbf{B}$ was constructed from the atomic polarizabilities and their dipolar interactions. A molecular polarizability of 7.7 Å³ was calculated for HCBrClF; this is comparable to a value of 7.8 Å³ reported by Applequist.[29] The differences in these values are probably due to differences in the atomic coordinates used in the two calculations.

The residuals of the Raman scattering parameters, defined as $[\bar{\alpha}'^2_{obsd} - \bar{\alpha}'^2_{calcd}]$ and $[\rho(obsd) - \rho(calcd)]$, were chosen to guide the least-squares optimization process. Optimization was carried out on a Univac 1110 computer using the subroutine ZXSSQ[30] with the strict descent option. Three stages were used in the optimization. In the first stage, the six independent components of each $\nabla_X \alpha_i$ tensor were allowed to oscillate until the residuals in successive iterations did not improve. The resulting values were taken as starting parameters for the second stage where the diagonal elements alone were permitted to vary. The least-squares fit proceeded until the residuals in successive cycles showed no further improvement. At this point, all second-stage component values were placed into the Jacobian matrix for final optimization. Consistent improvement in the fit was achieved in each successive stage of this process.

Initially, it was our intention to relax the symmetric constraint on the $\nabla_X \alpha_i$ tensors. However, after consideration of the number of available experimental parameters and the uncertainty concerning the proper stage at which to introduce the asymmetry, it was decided that relaxation of the symmetric constraint is presently impractical. Furthermore, any ambiguities in the force field and thereby in the normal coordinates will be transmitted to the atomic polarizability derivative components. Diem and Burow[18] have noted some significant differences in the vibrational mode descriptions as obtained from general valence (GVFF) and Urey–Bradley (UBFF) force field treatments. In order to investigate the effects of different force fields, the optimization was performed utilizing $\mathbf{L}$ matrices obtained from both GVFF[17] and UBFF[18] descriptions.

In Table III, the experimental values of $\bar{\alpha}'^2$ and ρ are compared with the corresponding calculated values. The standard deviations in $\bar{\alpha}'^2$ and ρ are 0.10 Å⁴ amu⁻¹ and 0.18, respectively, with the UBFF whereas they are 0.12 Å⁴ amu⁻¹ and 0.19, respectively, with the GVFF. For the UBFF treatment, the major contribution to the residual in ρ is from ν_3. This situation could have been anticipated for several reasons: there

Table III. Comparison between Observed and Calculated Raman Scattering Parameters for Bromochlorofluoromethane

| | polarizability derivative $\overline{\alpha}'^{2\,a}$ | | | | | depolarization ratio ρ | | | | |
| | | calcd | | difference | | | calcd | | difference | |
	obsd	UBFF	GVFF	UBFF	GVFF	obsd	UBFF	GVFF	UBFF	GVFF
					HCBrClF					
ν_1	0.75_7	0.75_6	0.75_0	0.00	0.00	0.12	0.32	0.31	−0.20	−0.19
ν_2	0.01_7	0.15_1	0.14_6	−0.13	−0.13	0.40	0.47	0.70	−0.07	−0.30
ν_3	$0.01_0{}^b$	0.20_6	0.22_7	−0.19	−0.21	0.30	0.67	0.54	−0.37	−0.24
ν_4	0.14_0	0.18_5	0.15_2	−0.04	−0.01	0.58	0.54	0.59	0.03	−0.01
ν_5	0.23_8	0.43_3	0.50_8	−0.19	−0.27	0.61	0.63	0.62	−0.02	−0.01
ν_6	0.23_1	0.31_3	0.35_2	−0.08	−0.12	0.06	0.11	0.18	−0.05	−0.13
ν_7	0.07_4	0.08_4	0.06_3	−0.01	0.01	0.07	0.18	0.10	−0.12	−0.03
ν_8	0.01_6	0.10_8	0.10_3	−0.09	−0.08	0.24	0.41	0.31	−0.17	−0.08
ν_9	0.02_2	0.10_3	0.11_4	−0.08	−0.09	0.23	0.31	0.28	−0.08	−0.05
					DCBrClF					
ν_1	$0.5_8{}^b$	0.66_6	0.58_5	−	−	0.12	0.19	0.21	−0.08	−0.09
ν_2	$0.1_8{}^b$	0.34_3	0.01_5	−	−	0.15	0.30	0.74	−0.15	−0.59
ν_3	$0.1_3{}^b$	0.00_6	0.38_5	−	−	0.24	0.74	0.38	−0.50	−0.14
ν_4	0.21_4	0.20_4	0.25_3	0.01	−0.04	0.40	0.52	0.62	−0.12	−0.23
ν_5	0.60_4	0.46_6	0.45_1	0.13	0.15	0.35	0.51	0.54	−0.16	−0.19
ν_6	0.11_3	0.10_8	0.17_2	0.00	−0.06	0.09	0.18	0.20	−0.09	−0.11
ν_7	0.04_7	0.08_8	0.06_0	−0.04	−0.01	0.07	0.19	0.12	−0.12	−0.05
ν_8	0.01_1	0.11_1	0.10_2	−0.10	−0.09	0.29	0.40	0.32	−0.11	−0.03
ν_9	0.02_2	0.08_5	0.11_5	−0.06	−0.09	0.24	0.36	0.28	−0.12	−0.04

a The units of $\overline{\alpha}'^2$ are $\text{Å}^4\,\text{amu}^{-1}$. *b* These values have considerable uncertainty (see text).

Table IV. Cartesian Derivatives of the Atomic Polarizability Tensor Components for Bromochlorofluoromethane[a]

i	$\partial\alpha_i{}^{xx}/\partial x_i$	$\partial\alpha_i{}^{yy}/\partial y_i$	$\partial\alpha_i{}^{zz}/\partial z_i$	$\partial\alpha_i{}^{xx}/\partial y_i$	$\partial\alpha_i{}^{xx}/\partial z_i$	$\partial\alpha_i{}^{yy}/\partial z_i$
H	−0.678	−6.026	7.693	0.094	−0.062	−2.269
C	6.036	−2.859	0.122	0.488	−0.071	0.343
F	−7.231	−0.806	−48.346	2.013	6.522	1.281
Cl	−13.593	−2.621	0.215	11.921	7.917	−1.902
Br	44.844	−8.130	−4.398	2.818	9.032	−7.655

a These values, in units of Å^2, were optimized using the Raman scattering parameters and the Urey–Bradley force field as discussed in the text.

is a general ambiguity in the assignment of ν_2 and ν_3, experimental parameters for ν_3 are uncertain in HCBrClF owing to Fermi resonance with $\nu_5 + \nu_7$, and $\overline{\alpha}'^2$ for ν_3 in DCBrClF was not involved in the optimization process. Upon removal of the residual in ρ for ν_3, the standard deviation in ρ for the UBFF becomes 0.11. In contrast to the situation with the UBFF, the GVFF description has major contributions to the residual from several modes.

Upon examination of Table III, several features become apparent. First of all, the fit is remarkably good when examined with a perspective which includes the complexity of the vibrational problem in HCBrClF as well as the quality of the fit achieved for the totally symmetric modes of simple halomethanes by Applequist and Quicksall.[20] The standard deviation in the $\overline{\alpha}'^2$ values is roughly half that achieved by Applequist and Quicksall.[20] Admittedly, our sample basis is not as diverse as that of Applequist and Quicksall, but the vibrational problem is more complex, especially when *all* molecular vibrational modes must be involved. These observations suggest that the ADl model can, indeed, be employed in a realistic, legitimate, and effective fashion for the evaluation of the Raman scattering parameters of simple chiral molecules. Closer inspection reveals that the calculated values of both the mean polarizability derivatives and the depolarization ratios are consistently somewhat high with both force fields. The largest relative discrepancies in $\overline{\alpha}'^2$ occur in ν_2, ν_3, ν_8, and ν_9 where the observed $\overline{\alpha}'^2$ values are small; thus the residual criterion for achieving a good fit is less effective in reducing the discrepancy than in the other modes. The predicted mean polarizability derivatives are, uniformly, similar for both force fields with the exception of ν_2 and ν_3 of DCBrClF; in the latter

two modes, the factors cited in the previous paragraph are undoubtedly involved. As expected from the results of Applequist and Quicksall,[20] the predicted $\overline{\alpha}'^2$ values are better than the depolarization ratios. The moderately large absolute discrepancy in $\overline{\alpha}'^2$ for ν_5 can be attributed to the large difference in the observed values of $\overline{\alpha}'^2$ for ν_5 in the two isotopic molecules.

Comparison of the normal coordinate derivatives of the molecular polarizability tensors, α'_{mol}, revealed that with the GVFF description, but not with the UBFF description, a sign change for $\overline{\alpha}'(\nu_{C-H})$ occurs upon isotopic substitution. In general, upon isotopic substitution a change in magnitude but not in sign may be expected for an internal mode which is virtually not coupled with other internal modes. A similar comparison of α'_{mol} values in the other normal modes reveals a similar favorable bias toward the UBFF. Since the UBFF description also provides smaller standard deviations in $\overline{\alpha}'^2$ and ρ, it is apparent that the UBFF is preferable to the GVFF at this point. In view of these merits, the final, optimized set of $\nabla_X\alpha_i$ tensor components is reported only for the UBFF description (Table IV); the corresponding molecular polarizability derivative tensors for the normal vibrations are given in Table V.

It is useful to compare the $\partial\alpha_i/\partial R_i$ values obtained from these optimized $\nabla_X\alpha_i$ values with those reported earlier. Applequist and Quicksall[20] optimized the $\partial\alpha_i/\partial R_i$ values with the assumption that $\partial\alpha_i/\partial R_i$ vanishes unless R_i is a stretching coordinate containing the atom i. With these approximations, Applequist and Quicksall obtained values of 0.75, 1.1, 3.2, and 3.7 Å^2 for $\partial\alpha_H/\partial R_{C-H}$, $\partial\alpha_F/\partial R_{C-F}$, $\partial\alpha_{Cl}/\partial R_{C-Cl}$, and $\partial\alpha_{Br}/\partial R_{C-Br}$, respectively. The corresponding values obtained

Table V. Normal Coordinate Derivatives of the Molecular Polarizability Tensor Components for Bromochlorofluoromethane[a]

	α'_{xx}	α'_{yy}	α'_{zz}	α'_{xy}	α'_{xz}	α'_{yz}
			HCBrClF			
ν_1	2.29	0.496	−0.177	−0.680	−0.209	0.115
ν_2	0.186	−0.607	−0.746	0.834	0.187	0.099
ν_3	−0.254	−0.773	2.390	0.601	−1.627	0.721
ν_4	−0.392	0.507	1.175	−0.712	0.049	−0.868
ν_5	−0.263	−1.713	0.002	0.445	−1.075	2.588
ν_6	0.305	0.366	1.009	−0.046	0.254	−0.016
ν_7	0.321	0.344	0.206	−0.193	0.225	−0.117
ν_8	−0.223	−0.235	−0.531	−0.382	−0.519	−0.212
ν_9	0.385	0.180	0.402	−0.038	0.511	0.092
			DCBrClF			
ν_1	1.708	0.563	0.178	−0.508	−0.122	0.016
ν_2	−0.072	0.559	1.270	−0.586	−0.239	−0.084
ν_3	−0.096	−1.576	1.428	0.717	−1.641	2.034
ν_4	0.387	−0.393	−1.350	0.616	0.099	0.760
ν_5	−0.319	−1.150	−0.580	0.213	−0.500	1.840
ν_6	0.251	0.211	0.523	0.014	0.315	0.054
ν_7	0.306	0.371	0.214	−0.196	0.231	−0.132
ν_8	−0.212	−0.249	−0.541	−0.381	−0.525	−0.195
ν_9	0.390	0.146	0.339	−0.040	0.517	0.121

[a] These values, in units of Å^2 $\text{amu}^{-1/2}$, were obtained with the Urey–Bradley force field by the procedure outlined in the text.

from the optimized $\nabla_X \alpha_i$ components in the present investigation are −0.01, −1.9, 0.4, and 1.05 Å^2, respectively. The reason for the differences between the present values and those of Applequist and Quicksall is easily understood. In the present calculations, none of the $\partial \alpha_i / \partial R_l$ values was neglected whereas they were considered to be negligible by Applequist and Quicksall. For example, it is found that large interactions between fluorine and the other halogen atoms occur; these interactions are reflected by the parameters $\partial \alpha_F / \partial R_{C\text{-}Br}$, $\partial \alpha_F / \partial \phi_{FCBr}$, and $\partial \alpha_F / \partial \phi_{FCCl}$, which have the values −7.66, −8.13, and 5.99 Å^2, respectively. This observation demonstrates that optimization of $\nabla_X \alpha_i$ components, in addition to possessing other distinct advantages, is the most appropriate route to α'_{mol}.

The components of the Raman circular intensity differential, polarized perpendicular (s) and parallel (p) to the scattering plane were evaluated from the following equations using the optimized $\nabla_X \alpha_i$ tensors and the procedures described earlier.[16]

$$\Delta_s(Q_k) = \frac{4\pi}{n\lambda_e} \frac{7\alpha'_{\alpha\beta}\beta'_{\alpha\beta} + \alpha'_{\alpha\alpha}\beta'_{\beta\beta} + \frac{1}{3}\alpha'_{\alpha\beta}\epsilon_{\alpha\gamma\delta}A'_{\gamma\delta\beta}}{7\alpha'_{\lambda\mu}\alpha'_{\lambda\nu} + \alpha'_{\lambda\lambda}\alpha'_{\mu\mu}}$$

(11)

$$\Delta_p(Q_k) = \frac{4\pi}{n\lambda_e} \frac{3\alpha'_{\alpha\beta}\beta'_{\alpha\beta} - \alpha'_{\alpha\alpha}\beta'_{\beta\beta} - \frac{1}{3}\alpha'_{\alpha\beta}\epsilon_{\alpha\gamma\delta}A'_{\gamma\delta\beta}}{3\alpha'_{\lambda\mu}\alpha'_{\lambda\mu} - \alpha'_{\lambda\lambda}\alpha'_{\mu\mu}}$$

(12)

Here $\alpha'_{\alpha\beta}$, $\beta'_{\alpha\beta}$, and $A'_{\alpha\beta\gamma}$ represent the components of the normal coordinate derivatives of molecular polarizability, rotatory polarizability, and quadrupole polarizability tensors; n is the refractive index of the medium, and λ_e is the wavelength of the exciting radiation. Values for the individual tensor components, $\alpha'_{\alpha\beta}$, were those obtained from the treatment described above. Values for the corresponding components of the other tensors, $\beta'_{\alpha\beta}$ and $A'_{\alpha\beta}$, were obtained from the optimized $\nabla_X \alpha_i$ components by the procedure described earlier.[16]

The predicted values of the Raman CIDs of (R)-HCBrClF and (R)-DCBrClF using both GVFF and UBFF treatments are summarized in Table VI. The separate contributions of the

$\alpha'\beta'$ and $\alpha'A'$ products are presented in Table VII for the UBFF treatment; values with a similar pattern were also obtained for the GVFF treatment. A parallel computation with the opposite enantiomer produced equal values of opposite sign for all components. All Raman CIDs were evaluated with λ_e 589 nm and $n = 1.414$ (eq 11 and 12) so as to approximate liquid-phase values (vide infra); CIDs for other excitation wavelengths can be obtained by use of appropriate values for n and λ_e. No appreciable error is expected from use of $\alpha'_{\alpha\beta}$, $\beta'_{\alpha\beta}$, and $A'_{\alpha\beta\gamma}$ terms evaluated at 488 nm in this case since dispersion in the visible region of the spectrum is small.

Several important observations can be made concerning the predicted Raman CIDs given in Table VI. First, all CIDs are of the proper order of magnitude (10^{-3}–10^{-5}) compared with CIDs reported for other molecules.[3-8] Secondly, it is remarkable that the GVFF and the UBFF are both quite consistent in their predictions of relative magnitudes and signs of the CIDs. It is apparent that the GVFF predicts somewhat larger CIDs than does the UBFF. When allowance is made for the fact that ν_2 and ν_3 have virtually interchanged mode descriptions in the two force fields, only with $\nu_1(\Delta_p)$, $\nu_7(\Delta_s)$, and $\nu_9(\Delta_s)$ are the signs not the same, and here ν_1 and ν_9 have such small CIDs that the significance of the sign difference is questionable. Thirdly, both force fields predict the larger CIDs to be in deformation modes; this is also consistent with observations reported[3-8] for other molecules. The UBFF results may be more reliable than the GVFF results since the UBFF gives better Raman scattering parameters. However, no strong case can be made either in favor of one or against the other treatment.

It is apparent that the computed contributions of the $\alpha'\beta'$ and $\alpha'A'$ terms (Table VII) to the CIDs are of the same order of magnitude as predicted by theory.[1] It is interesting that the $\alpha'\beta'$ and $\alpha'A'$ terms generally have the same sign; the only exceptions are ν_7 and ν_9 with the UBFF treatment. As a consequence, Δ_s is predicted to be somewhat larger than Δ_p in spite of the smaller overall scattering intensity in the p polarized component; this situation arises because Δ_s contains a positive interference between $\alpha'\beta'$ and $\alpha'A'$ contributions whereas Δ_p contains a negative interference of these contributions (see eq 11 and 12). Inspection of Table VII also reveals that the $\alpha'A'$ contribution, although of the same order of magnitude as the $\alpha'\beta'$ contribution, is distinctly smaller than the $\alpha'\beta'$ contribution. Thus it would appear that qualitative evaluation of the magnitude and sign pattern could be obtained from a consideration of the $\alpha'\beta'$ terms alone.

Direct comparison with experimental observations on optically active HCBrClF would be invaluable, but, despite some encouraging parallels between our calculated results and our preliminary observations, the measurements are not presently reliable enough for detailed discussion. It should also be recognized that comparison with only the Δ_p component would be practical since the other component is not free of artifact. According to UBFF predictions, with an optically pure sample, four modes (ν_6–ν_9) and possibly also ν_2 and ν_3 would have a Δ_p of sufficient magnitude for reliable measurement with present instrumentation; these same modes would also be observable according to the GVFF predictions. The larger CIDs could probably be observed even with a sample of 20–30% optical purity or with a 25% sample in an inert solvent.

An interesting comparison can be made with the substituent-mass equivalent molecule, α-phenylethyl isocyanate. The skeletal modes of α-phenylethyl isocyanate,[31] which occur at 223, 313, and 345 cm^{-1}, are probably roughly equivalent to the ν_9, ν_8, and ν_7 modes of HCBrClF, which occur at 229, 318, and 431 cm^{-1}, respectively. The values of Δ_p for the 223-, 313-, and 345-cm^{-1} modes of $(-)$-α-phenylethyl isocyanate are reported[31] to be ca. -2.0×10^{-3}, $+1.7 \times 10^{-3}$, and -0.3×10^{-3}, respectively; the corresponding (UBFF) values of ν_9, ν_8,

Table VI. Predicted Raman Circular Intensity Differentials[a] for (R)-HCBrClF and (R)-DCBrClF

		UBFF			GVFF		VCD[b]
	mode	$\Delta_s \times 10^3$	$\Delta_p \times 10^3$	mode	$\Delta_s \times 10^3$	$\Delta_p \times 10^3$	$G \times 10^5$
				HCBrClF			
ν_1	$\nu_{C\text{-}H}$	0.05	-0.00_3	$\nu_{C\text{-}H}$	0.18	0.02	-0.05
ν_2	$\delta_{HCF} + \delta_{HCBr}$	-0.14	-0.13	$\delta_{HCCl} + \delta_{HCF}$	0.73	0.44	-1.1
ν_3	$\delta_{HCCl} + \delta_{HCBr}$	0.64	0.18	$\delta_{HCF} + \delta_{HCBr}$	-0.32	-0.35	$+5.0$
ν_4	$\nu_{C\text{-}F}$	0.09	0.06	$\nu_{C\text{-}F}$	0.07	-0.00	-1.7
ν_5	$\nu_{C\text{-}Cl} + \nu_{C\text{-}Br}$	-0.19	-0.06	$\nu_{C\text{-}Cl} + \delta_{FCCl}$	-0.23	-0.16	$+0.51$
ν_6	$\nu_{C\text{-}Br} + \nu_{C\text{-}Cl}$	-0.03	-0.38	$\nu_{C\text{-}Br} + \delta_{FCBr} + \delta_{ClCBr}$	-0.14	-0.16	-0.26
ν_7	δ_{FCCl}	0.17	-0.55	δ_{FCCl}	-0.76	-1.75	$+0.74$
ν_8	$\delta_{FCBr} + \nu_{C\text{-}Br}$	3.15	0.73	$\delta_{FCBr} + \nu_{C\text{-}Br}$	2.73	0.61	-1.4
ν_9	δ_{ClCBr}	0.00	-0.34	$\delta_{ClCBr} + \delta_{FCCl}$	0.09	-0.53	-1.1
				DCBrClF			
ν_1	$\nu_{C\text{-}D}$	0.03	-0.00_7	$\nu_{C\text{-}D}$	0.15	0.03	-1.4
ν_2	$\delta_{DCF} + \delta_{DCBr}$	-0.06	-0.25	$\delta_{DCCl} + \nu_{C\text{-}F} + \delta_{DCBr}$	0.29	0.23	-8.7
ν_3	$\delta_{DCCl} + \delta_{DCBr}$	0.39	0.23	$\delta_{DCF} + \delta_{DCBr}$	-0.04	-0.32	$+4.3$
ν_4	$\nu_{C\text{-}F}$	0.03	-0.00	$\nu_{C\text{-}F} + \delta_{C\text{-}Cl}$	0.17	0.17	$+2.3$
ν_5	$\nu_{C\text{-}Cl} + \nu_{C\text{-}Br}$	-0.37	-0.29	$\nu_{C\text{-}Cl}$	-0.42	-0.36	$+0.66$
ν_6	$\nu_{C\text{-}Br} + \delta_{ClCBr}$	-0.47	-0.87	$\nu_{C\text{-}Br} + \delta_{DCBr} + \delta_{FCBr}$	-0.52	-0.36	-0.39
ν_7	δ_{FCCl}	0.16	-0.49	δ_{FCCl}	-0.91	-1.81	$+0.75$
ν_8	$\delta_{FCBr} + \nu_{C\text{-}Br}$	3.14	0.73	$\delta_{FCBr} + \nu_{C\text{-}Br}$	2.72	0.60	-1.4
ν_9	δ_{ClCBr}	-0.05	-0.33	$\delta_{ClCBr} + \delta_{FCCl}$	0.06	-0.53	-1.1

[a] Raman CIDs were computed for $\lambda_e = 5893$ Å and $n = 1.414$ (eq 11 and 12). [b] For comparison, the vibrational circular dichroism G factors for (R)-HCBrClF, predicted from a fixed partial charge model and an anharmonic GVFF (ref 14), are illustrated. In a private communication, the authors indicated that their calculation (ref 14) utilized the S configuration.

and ν_7 for (R)-HCBrClF are -0.34×10^{-3}, $+0.73 \times 10^{-3}$, and -0.55×10^{-3}, respectively; a similar sign pattern is also predicted by the GVFF. It is highly encouraging that the relative sign pattern of these α-phenylethyl isocyanate modes is equivalent to both the UBFF and GVFF descriptions.

Inspection of the differences predicted for the two isotopic molecules reveals that both would be expected to have roughly equivalent ROA spectra. Furthermore, the differences predicted by the two force fields are equivalent. The major differences occur in ν_2 and ν_3, which involve H/D motion, and in ν_5 and ν_6, where the mode composition changes upon isotopic substitution. Furthermore, the C–H/C–D deformation modes show a more marked change than does the C–H/C–D stretching mode. This prediction is also consistent with observations of the ROA of $[\alpha$-$^2H]$benzyl alcohol[32] where the C–D deformation modes but not the C–D stretching modes exhibit significant Δ_p values.

It is interesting to compare these Raman CID results with equivalent predictions of the infrared VCD. The infrared VCD dissymmetry factors, as predicted by Marcott et al.,[14] using a fixed partial charge model and an anharmonic GVFF (derived from our harmonic GVFF[17]), are, therefore, illustrated in Table VI. First of all, it is apparent that the VCD G factors are some one to two orders of magnitude smaller than the Raman CIDs. This is consistent with reports in the literature where CIDs are generally 10^{-3}–10^{-4} [3-8] and G factors are generally[2,10] 10^{-5}–10^{-6}. Secondly, with bromochlorofluoromethane in *both* VCD and ROA, the larger effects are found in deformation rather than in stretching modes. Finally, there is no consistent trend in the relative signs of the two effects nor is there any apparent parallel or inverse relationship among the magnitudes of the two chiroptical parameters. This is not surprising since the two effects arise from physically different interactions.

Although it is pleasing to note the remarkable results achieved by these calculations, it is prudent to recognize that distinct limitations are present and that significant improvements are required in the future. With respect to the α'_{mol} components, it is apparent that refinement in the optimization procedures for $\nabla_\chi \alpha_i$ is necessary to achieve the potential transferability. This transferability should be practical when

Table VII. Predicted $\alpha'\beta'$ and $\alpha'A'$ Contributions to the Raman Circular Intensity Differentials for (R)-HCBrClF and (R)-DCBrClF Using the UBFF

	$\Delta_s \times 10^3$		$\Delta_p \times 10^3$	
	$\alpha'\beta'$	$\alpha'A'$	$\alpha'\beta'$	$\alpha'A'$
	contri-	contri-	contri-	contri-
mode	bution[a]	bution[b]	bution	bution
		HCBrClF		
ν_1	0.04	0.00_6	0.02	0.02
ν_2	-0.01	-0.13	-0.54	-0.41
ν_3	0.54	0.10	0.44	0.26
ν_4	0.09	0.00	0.07	0.01
ν_5	-0.14	-0.05	-0.18	-0.12
ν_6	-0.02	-0.01	-0.47	-0.09
ν_7	0.26	-0.09	-1.12	-0.57
ν_8	2.68	0.47	2.37	1.63
ν_9	0.07	-0.07	-0.63	-0.29
		DCBrClF		
ν_1	0.03	0.00	0.01	0.02
ν_2	0.03	-0.09	-0.63	-0.38
ν_3	0.34	0.05	0.35	0.12
ν_4	0.04	0.00	-0.02	-0.01_7
ν_5	-0.29	-0.08	-0.53	-0.23
ν_6	-0.42	-0.05	-1.20	-0.33
ν_7	0.24	-0.08	-1.01	-0.52
ν_8	2.66	0.47	2.37	1.64
ν_9	0.03	-0.08	-0.63	-0.30

[a] The $\alpha'\beta'$ contribution corresponds to the value of the first two terms in eq 11 and 12. [b] The $\alpha'A'$ contribution corresponds to the value of the third term in eq 11 and 12.

no major approximations are involved in evaluation of $\nabla_\chi \alpha_i$. Thus the approximation that the $\nabla_\chi \alpha_i$ tensors are symmetric will need to be removed so that all independent elements of the tensor are optimized. In the present situation, even if values for $\bar{\alpha}'_{mol}$ were available for ν_1, ν_2, and ν_3 of DCBrClF, an insufficient number of observables would have been available. Furthermore, since optimization was carried out on $\bar{\alpha}'_{mol}{}^2$ values, an ambiguity in the sign of $\bar{\alpha}'_{mol}$ is unavoidable; unfortunately there is no reliable procedure for verification of the resultant signs of the optimized $\bar{\alpha}'_{mol}$ values. Thus no claim to

having generated a unique set of values is possible. Nevertheless, the set of $\nabla_\chi\alpha_i$ values is perhaps the best empirically justified set currently available and it will be an ideal initial set to be used for future optimizations which will include a much broader data base. Secondly, we have no way of knowing how well this ADI procedure models the rotatory polarizability and the electric quadrupole derivative tensors; unfortunately, there is no practical way, at present, of separately measuring either their individual or their irreducible components.

Another aspect to be considered is that reliable comparison of predicted and observed Raman CIDs requires a correction for the intermolecular interactions of the liquid phase because the calculated values are essentially those for a free molecule. Some information on the effect of these intermolecular interactions is available through a comparison of liquid- and gas-phase Raman scattering parameters. It is apparent that liquid-phase effects on $\overline{\alpha}'_{mol}$ are dependent on the type of normal mode and that these effects can apparently enter either directly or inversely (vide supra). Since the denominators of the expressions for Δ (eq 11 and 12) are proportional to the intensity, it would be possible to include medium effects in the denominator. Full incorporation of such effects, however, would require knowledge of the behavior of the *individual* elements of α'_{mol}, β'_{mol}, and A'_{mol}. Because such knowledge is not possible and partial correction is not justifiable, we had to be content with the naive attribution of all medium effects to the refractive index term in the CID expressions (eq 11 and 12). This correction would probably be appropriate for comparison with CIDs measured for a dilute solution of HCBrClF in an "inert" solvent, but significant deviations could occur upon comparison with CIDs measured with pure liquid HCBrClF. If medium effects on α'_{mol} were predominant in the latter case, our measurements of $\overline{\alpha}'^2_{liq}/\overline{\alpha}'^2_{vap}$ (Table I) would suggest three different categories of liquid-phase perturbation: ν_1 and ν_6, ν_4 and ν_5, and ν_2, ν_3, ν_7, ν_8, ν_9. On the other hand, if α'_{mol}, β'_{mol}, and A'_{mol} are affected more or less equally by the interactions, the medium effects on terms appearing in the numerator and denominator could cancel each other. The latter situation could be operative since the predicted magnitudes and signs roughly parallel those observed with liquid-phase α-phenylethyl isocyanate.

Conclusions

In summary, a powerful technique developed from an atom–dipole interaction model has provided the first calculation of Raman optical activity parameters. The method, applied to the very simple chiral molecule HCBrClF, produced results which are remarkably consistent in magnitude and relative sign with observations on molecules of similar structure. The observation that the GVFF and the UBFF both predict the same modes to have the major CIDs as well as equivalent signs despite significant differences in the force fields might suggest that *qualitatively* reliable predictions of ROA are possible even with force fields that are less than ideal. The results with HCBrClF are of general significance in that they serve as a model for the ROA of other molecules where motion about an asymmetrically substituted carbon atom occurs. These apparently successful efforts are sufficiently encouraging to justify exploration of a more approximate numerical version of the ADI method with molecules of higher complexity. Finally, since a link between molecular structural features and Raman CIDs is now available, it is timely to synthesize and/or resolve sets of simple chiral molecules where predictions of either the full or the numerical methods can be effectively tested. Progress made in several of these directions will be communicated shortly.

References and Notes

(1) L. D. Barron, *Adv. Infrared Raman Spectrosc.*, **4**, 271 (1977); L. D. Barron and A. D. Buckingham, *Annu. Rev. Phys. Chem.*, **26**, 381 (1975).
(2) L. A. Nafie, T. A. Keiderling, and P. J. Stephens, *J. Am. Chem. Soc.*, **98**, 2715 (1976).
(3) L. D. Barron, M. P. Bogaard, and A. D. Buckingham, *J. Am. Chem. Soc.*, **95**, 603 (1973).
(4) W. Hug, S. Kint, G. F. Bailey, and J. R. Scherer, *J. Am. Chem. Soc.*, **97**, 5589 (1975).
(5) L. D. Barron and A. D. Buckingham, *J. Chem. Soc., Chem. Commun.*, 152 (1973).
(6) L. D. Barron and A. D. Buckingham, *J. Chem. Soc., Chem. Commun.*, 1028 (1974); L. D. Barron, *J. Chem. Soc., Perkin Trans. 2*, 1074 (1977).
(7) H. Boucher, T. R. Brocki, M. Moskovits, and B. Bosnich, *J. Am. Chem. Soc.*, **99**, 6870 (1977).
(8) L. D. Barron, *Tetrahedron*, **34**, 607 (1978).
(9) M. Diem, M. J. Diem, B. A. Hudgens, J. L. Fry, and D. F. Burow, *J. Chem. Soc., Chem. Commun.*, 1028 (1976).
(10) G. Holzwarth, E. C. Hsu, H. S. Mosher, T. R. Faulkner, and A. Moscowitz, *J. Am. Chem. Soc.*, **96**, 251 (1974).
(11) T. A. Keiderling and P. J. Stephens, *Chem. Phys. Lett.*, **41**, 46 (1976).
(12) J. A. Schellman, *J. Chem. Phys.*, **58**, 2882 (1973).
(13) T. R. Faulkner, A. Moscowitz, G. Holzwarth, E. C. Hsu, and H. S. Mosher, *J. Am. Chem. Soc.*, **96**, 252 (1974).
(14) C. Marcott, T. R. Faulkner, A. Moscowitz, and J. Overend, *J. Am. Chem. Soc.*, **99**, 8169 (1977).
(15) T. A. Keiderling and P. J. Stephens, *J. Am. Chem. Soc.*, **99**, 8061 (1977).
(16) P. L. Prasad and D. F. Burow, *J. Am. Chem. Soc.*, preceding paper in this issue.
(17) M. Diem and D. F. Burow, *J. Chem. Phys.*, **64**, 5179 (1976).
(18) M. Diem and D. F. Burow, *J. Phys. Chem.*, **81**, 476 (1977).
(19) J. Applequist, J. R. Carl, and K. K. Fung, *J. Am. Chem. Soc.*, **94**, 2952 (1972).
(20) J. Applequist and C. O. Quicksall, *J. Chem. Phys.*, **66**, 3455 (1977).
(21) R. E. Hester in "Raman Spectroscopy: Theory and Practice", Vol. I, H. A. Szymanski, Ed., Plenum Press, New York, 1967, Chapter 4.
(22) T. Yoshino and H. J. Bernstein, *Spectrochim. Acta*, **14**, 127 (1959).
(23) B. Fontal and T. G. Spiro, *Spectrochim. Acta, Part A*, **33**, 507 (1977).
(24) G. Eckhardt and W. Wagner, *J. Mol. Spectrosc.*, **19**, 407 (1966); W. F. Murphy, W. Holzer, and H. J. Bernstein, *Appl. Spectrosc.*, **23**, 211 (1969).
(25) R. J. H. Clark and C. J. Willis, *Inorg. Chem.*, **10**, 1118 (1971).
(26) E. B. Wilson, J. C. Decius, and P. C. Cross, "Molecular Vibrations", McGraw-Hill, New York, N.Y., 1955.
(27) P. L. Prasad, *J. Chem. Phys.*, **69**, 4403 (1978); see also M. Gussoni, G. Dellipiane, and S. Abbate, *J. Mol. Spectrosc.*, **57**, 323 (1975); M. Gussoni and S. Abbate, *ibid.*, **62**, 53 (1976).
(28) Construction of the **C'** matrix involves terms such as $\partial r_{ij}/\partial Q$ which are obtained from the equation $\partial r_{ij}/\partial Q = \Delta DL$ (see eq 36 of the preceding article). These values correspond to the displacements of the unit mass molecule; therefore, **D** corresponds to the natural inverse of Wilson's **B** matrix. On the other hand, the **D** matrix as used in eq 9 corresponds to the usual mass dependent inverse. For details see ref 27. The inverse matrices were evaluated using the LPSDOR subroutine on the Univac 1110 (ref 30).
(29) J. Applequist, *J. Chem. Phys.*, **58**, 4251 (1973).
(30) International Mathematical and Statistical Libraries, Inc., Houston, Texas, Library 2, Vol. 2, 6th ed., 1977.
(31) L. D. Barron, M. P. Bogaard, and A. D. Buckingham, *Nature (London)*, **241**, 113 (1973). Note: Dr. L. D. Barron, in a private communication, indicated that the reported ROA spectra were attributed to the wrong enantiomers.
(32) L. D. Barron, *J. Chem. Soc., Chem. Commun.*, 305 (1977).